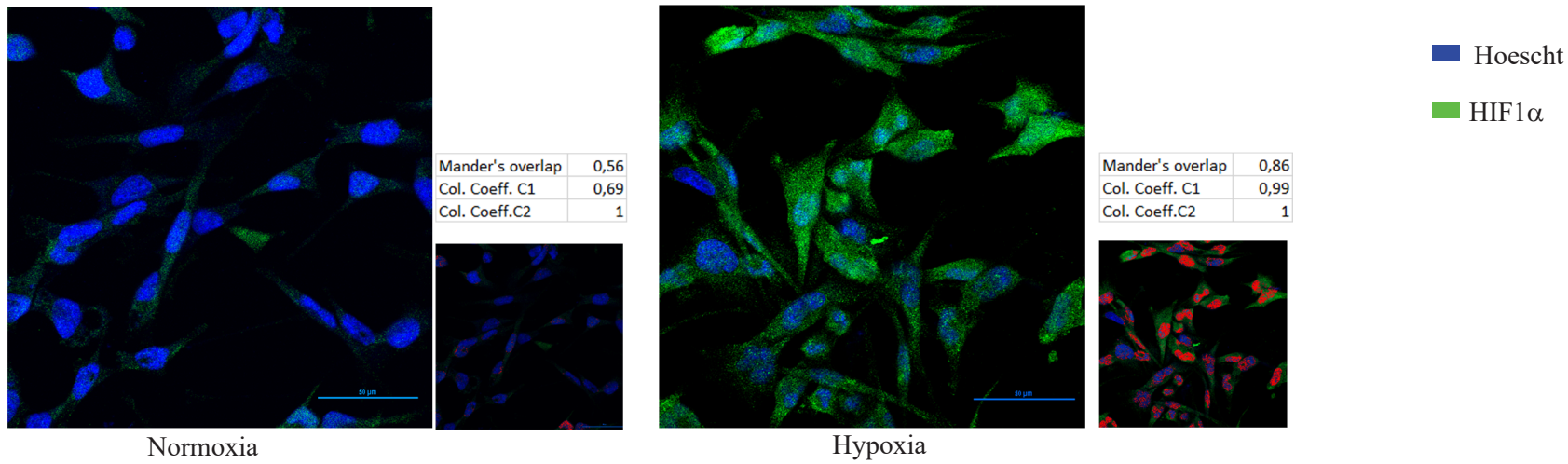


Supplementary information

S1



S2

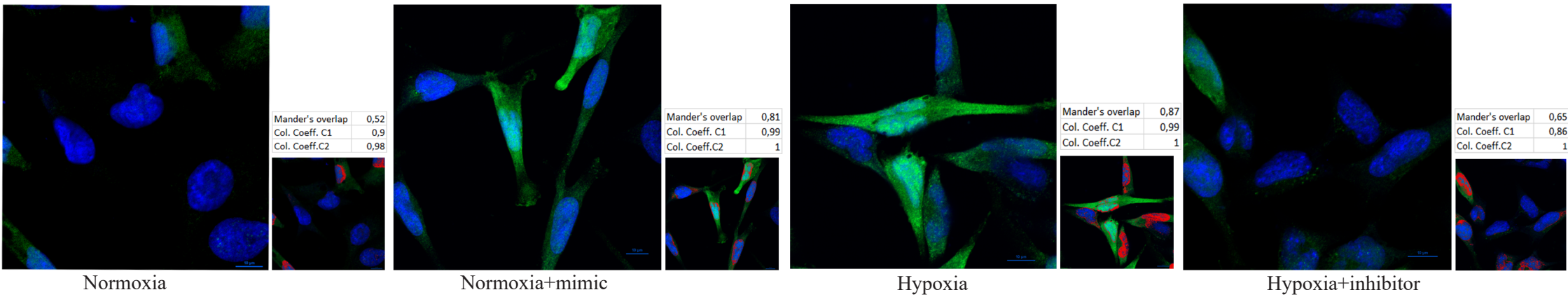


Figure S1

Medial focal plane of immunocytochemistry for HIF-1 α on U251 cells in hypoxic and normoxic conditions. HIF-1 α stained in green (FITC) and nuclei in blue (Hoescht). Scale bar 50 μ m. In the small squares co-localization analysis between Hoescht and FITC performed by NIS-Elements software (Nikon): co-localization pixels in red, relative Mander's overlap coefficients and colocalization coefficients are indicated in the figure.

Figure S2

Medial focal plane of immunocytochemistry for HIF-1 α on U251 cells in different culture conditions. HIF-1 α stained in green (FITC) and nuclei in blue (Hoescht). Scale bar 10 μ m. In the small squares co-localization analysis between Hoescht and FITC performed by NIS-Elements software (Nikon): co-localization pixels in red, relative Mander's overlap coefficients and colocalization coefficients are indicated in the figure.

Wst-1

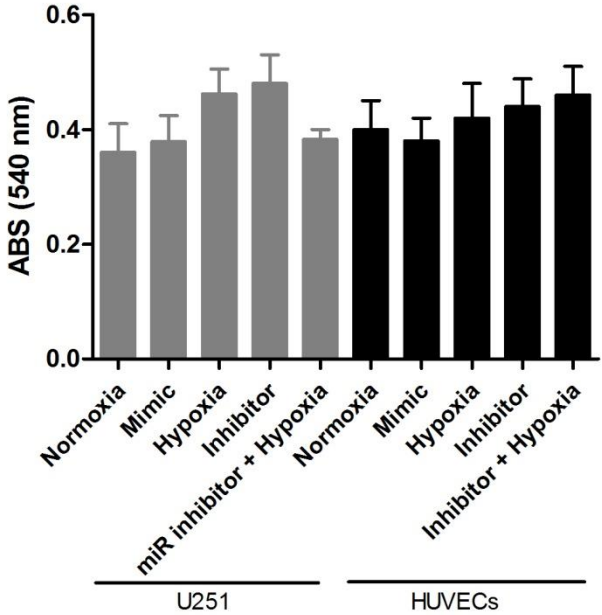


Figure S3. U251 cell viability evaluated by Wst-1 assay after mimic or inhibitor transfection. Data are represented as absorbance (540nm). Values are presented as the mean \pm SD.

S4

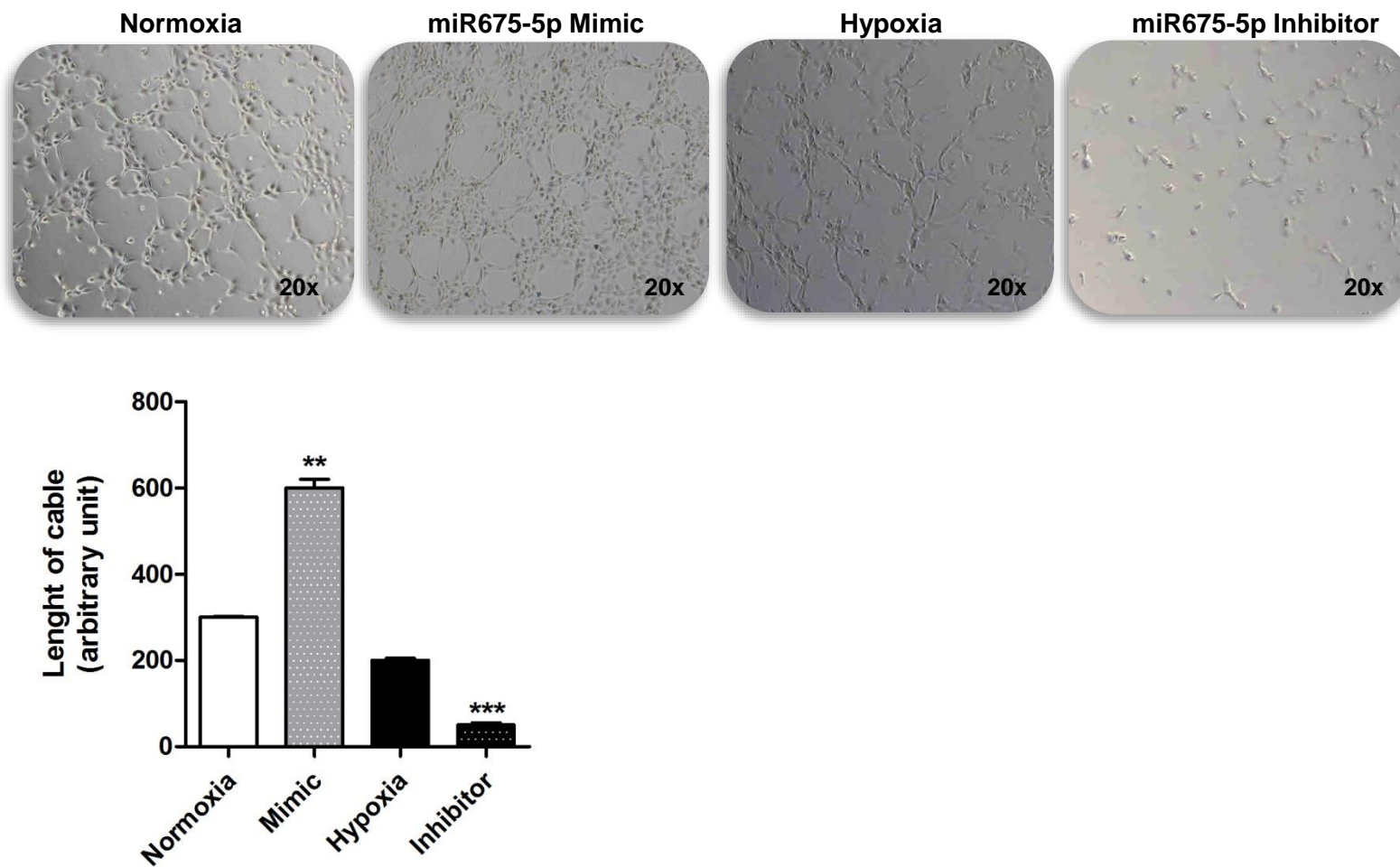


Figure S4. Phase contrast (20x) of tube formation assay of HUVECs in matrigel 2 hours after seeding (upper panel). The different conditions are indicated in the pictures. The graph (lower panel) represents the relative length of cable as arbitrary unit.

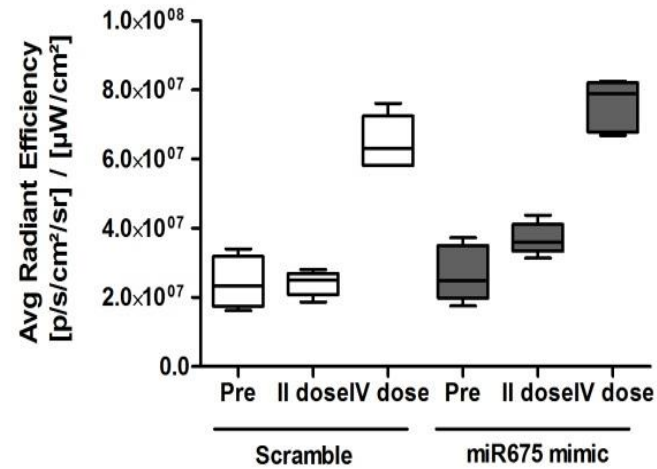
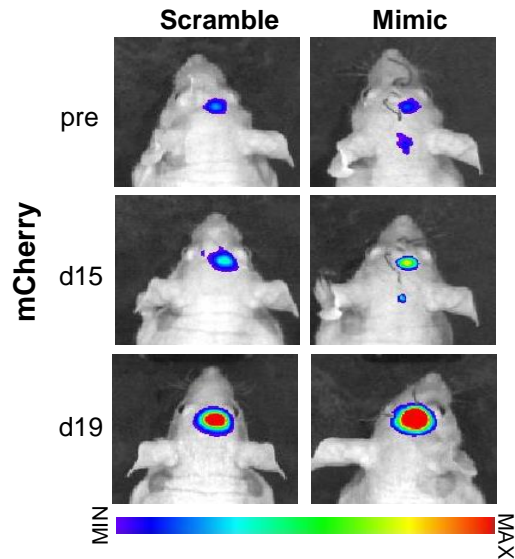


Figure S5. On the left panel, longitudinal mCherry fluorescent signal on representative scramble or mimic-treated mice at day 12 (pre-treatment), day 15 (after two i.v. administration) and day 19 (end of treatment). Images are presented with the same scale bar.

On the right panel, graphical representation of mCherry activity over time during treatment. Data are presented as average radiance efficiency [(photons/s/cm²/steradian)/(μW/cm²).

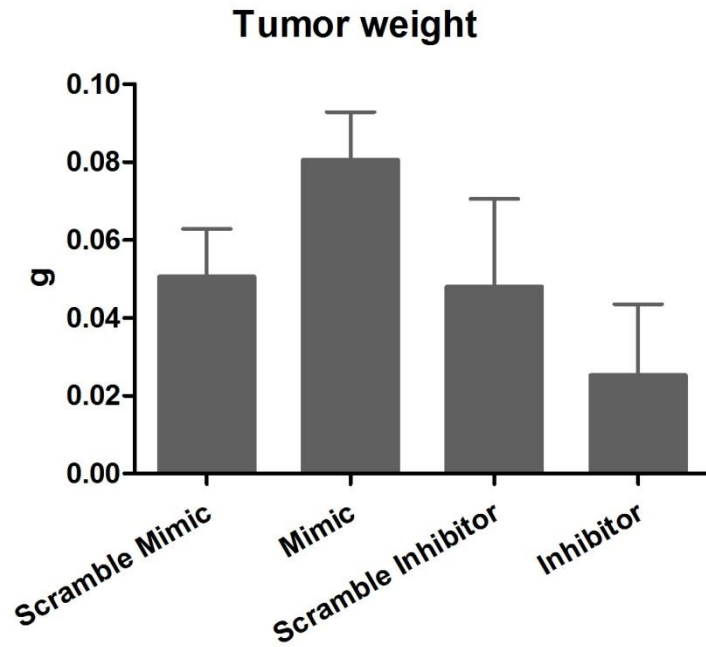


Figure S6. Tumor weight of *ex vivo* explantation harvested from mimic or inhibitor-treated mice and their relative scramble-treated mice (n=5 for each group). Values are presented as the mean \pm SD.

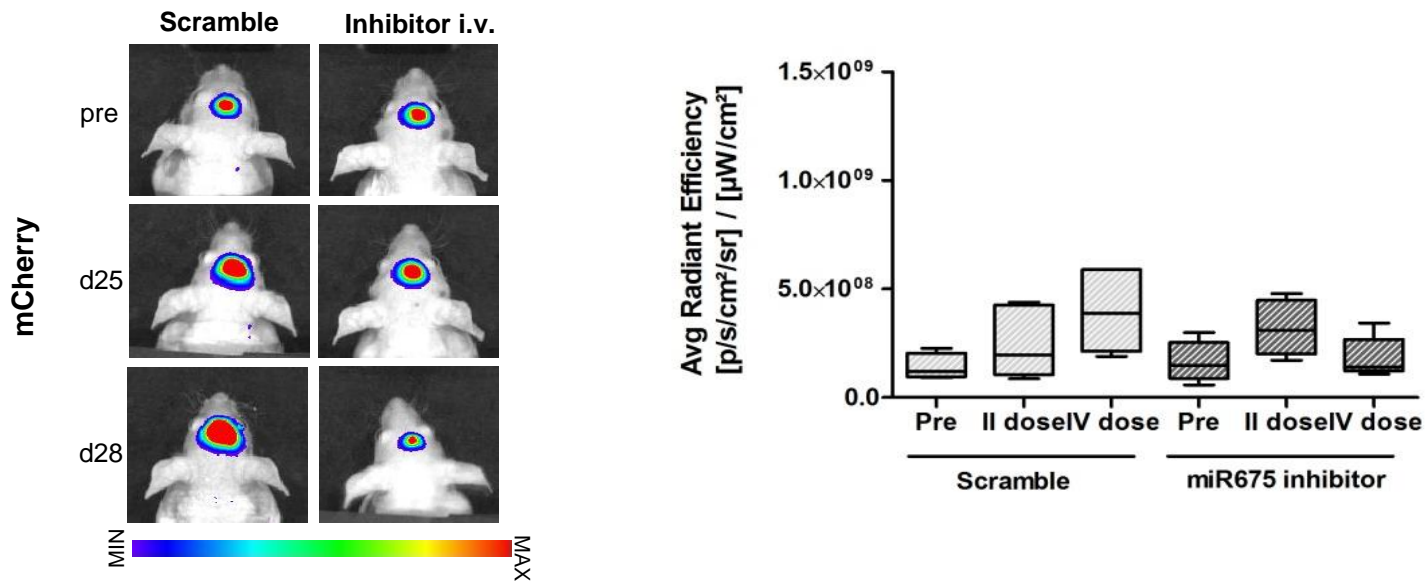


Figure S7. On the left panel, longitudinal mCherry fluorescent signal on representative scramble or inhibitor-treated mice at day21 (pre-treatment), day 25 (after two i.v. administration) and day 28 (end of treatment). Images are presented with the same scale bar.

On the right panel, graphical representation of mCherry activity over time during treatment. Data are presented as average radiance efficiency [(photons/s/cm²/steradian)/(μW/cm²).

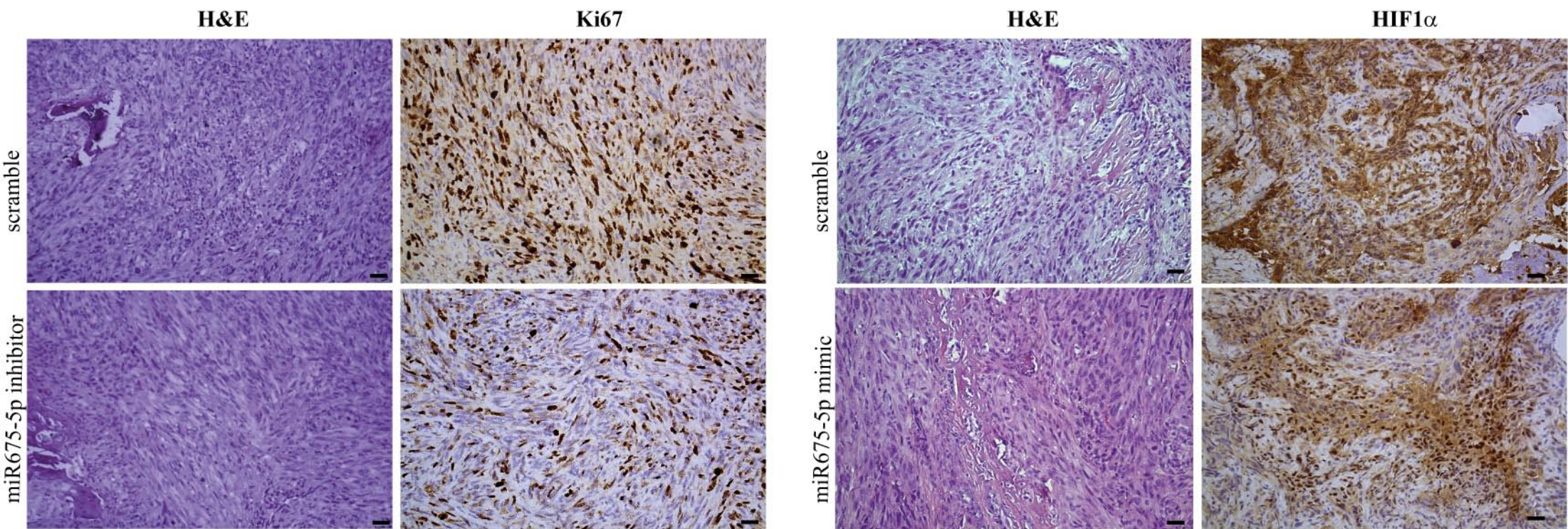


Figure S8. On the left, H&E and Ki67 staining performed at the end of miR675-5p inhibitor treatment(day 28). On the right, H&E and HIF-1 α performed at the end of miR675-5p mimic administration (day19). Scale bar 10 μ m.

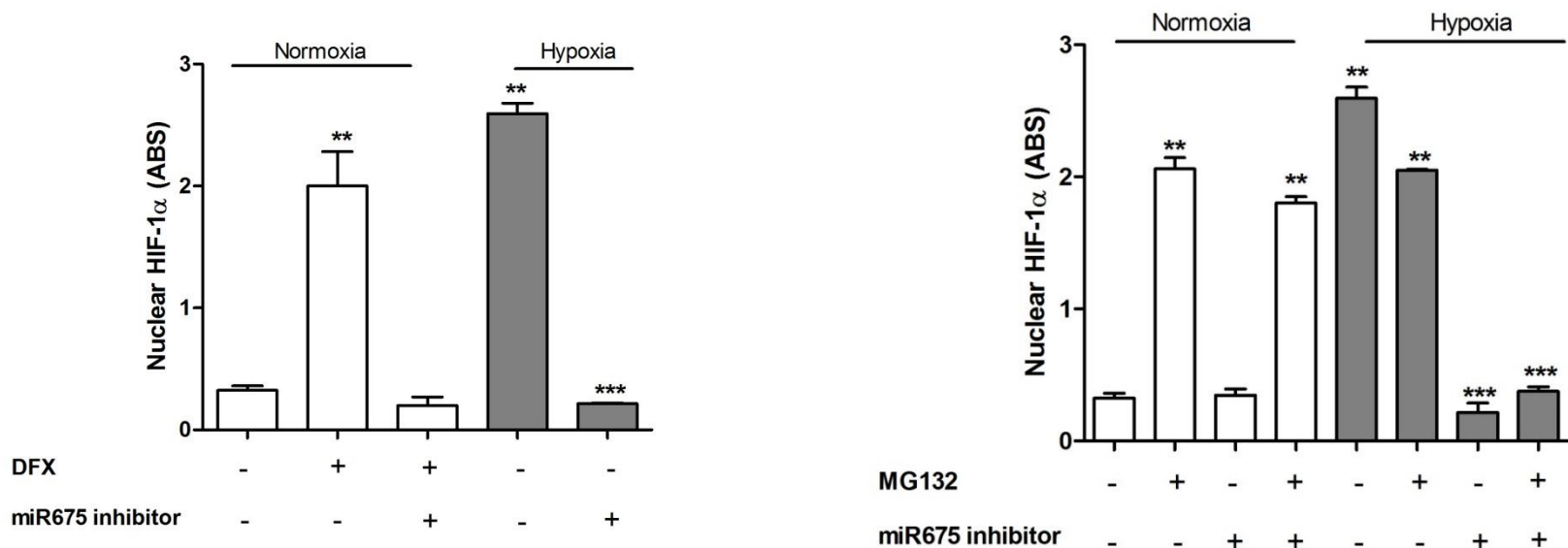


Figure S9. On the left panel, biochemical VHL inactivation performed through DFX treatment. U251 cells transfected with miRNA675-5p inhibitor were analyzed in normoxia \pm DFX and in hypoxia for HIF-1 α nuclear translocation. On the right panel, nuclear HIF-1 α was tested in U251 cells after treatment with proteasome inhibitor (MG132) \pm miRNA675-5p inhibitor, in normoxia and in hypoxia conditions. Data were expressed as ABS values at 450nm. Values are presented as the mean \pm SD, ** $p < 0.01$; *** $p < 0.001$.